

Is the peripapillary area completely healthy in Stargardt disease?

Ece Tuncel, Mehmet Çıtırık, Mevlüt Yılmaz

Department of Ophthalmology, Ankara Etlik City Hospital, Ankara, Türkiye

Cite this article: Tuncel E, Çıtırık M, Yılmaz M. Is the peripapillary area completely healthy in stargardt disease? *Ank Med J.* 2024;3(6):130-135.

Received: 29/08/2024

Accepted: 25/09/2024

Published: 13/11/2024

ABSTRACT

Aims: To evaluate the peripapillary retinal nerve fiber layer (pRNFL) thickness measured using spectral domain optical coherence tomography (SD-OCT) in patients with Stargardt disease (STGD).

Methods: This was a single-center, cross-sectional case-control study. Twenty eyes with STGD were staged according to Fishman STGD classification. Peripapillary RNFL thickness was measured using Heidelberg Spectralis SD-OCT. The mean pRNFL thickness of the four quadrants (temporal, superior, nasal, and inferior) and all quadrants were compared with the mean pRNFL thickness from 20 eyes of age-matched healthy subjects.

Results: The mean age of Stargardt patients was 40.9 years (range, 18–59 years) and that of the control group was 40.6 years (range, 19–59 years). Twenty eyes (70%) had thinner pRNFL thickness in the temporal quadrant (mean: $-7.55 \mu\text{m}$, 95%CI -3 to $-12 \mu\text{m}$, 10% thinner than the control group), whereas in the nasal quadrant, 13 of 20 eyes (65%) had thicker pRNFL (mean: $6.85 \mu\text{m}$, 95% CI, $1-13 \mu\text{m}$; 9% thicker compared to the control group). There was no statistically significant difference in the thickness of the superior and inferior quadrants and the global pRNFL compared to the control group.

Conclusion: STGD is considered pathognomonic for the preservation of the peripapillary retina and retinal pigment epithelium (RPE), and is mainly characterized by RPE and photoreceptor cell loss in the macula. STGD was associated with thinning of the temporal quadrant, corresponding to the macular area in the pRNFL analysis. It is not yet known whether the RNFL loss is due to transneuronal degeneration or direct damage to ganglion cells resulting from degeneration of the outer retinal layers.

Keywords: ABCA4, retinal nerve fiber layer, spectral-domain optical coherence tomography, Stargardt disease, transneuronal degeneration

INTRODUCTION

Stargardt disease (STGD) is the most common inherited macular dystrophy, with a prevalence of approximately 1 in 10,000.¹ In most patients, the inheritance pattern is autosomal recessive (AR), with the most commonly reported mutation occurring in the ABCA4 gene located on the short arm of chromosome 1 (1p22.1).² The ABCA4 gene encodes a transmembrane protein, a retina-specific adenosine triphosphate (ATP)-binding cassette transporter, which is localized to the rims of disc membranes in the outer segments of rod and cone photoreceptor cells and plays a critical role in retinoid recycling within the visual cycle. It functions as a retinoid translocase responsible for the active transport of N-retinylidene-phosphatidylethanolamine in the retinoid cycle, which facilitates the reduction of all-trans-retinal to all-trans-retinol by retinol dehydrogenase, thereby preventing side reactions that lead to the formation of toxic bisretinoid compounds.^{1,3} The loss of functional activity of the transporter leads to the accumulation of the retinoid intermediate N-retinylidene-phosphatidylethanolamine in the photoreceptor disc membranes, where it reacts with all-trans-

retinal to form phosphatidyl-pyridinium bisretinoid A2PE, the precursor of A2E, which abnormally accumulates in the retinal pigment epithelium (RPE).^{2,3} The accumulation of A2E, a major component of lipofuscin, in the RPE is toxic and leads to RPE dysfunction through complement activation, which subsequently causes photoreceptor degeneration.^{3,4}

In STGD, while the age of onset and progression varies among individuals, most patients typically experience significant bilateral loss of visual acuity, central scotoma, delayed dark adaptation, abnormal color vision during the early part of the first or second decade of life, and progressive central vision loss throughout their lives.^{1,4} Yellow-white flecks within the RPE around the macula and mid-peripheral retina, along with macular degeneration showing a beaten-bronze or bull's-eye appearance due to progressive RPE atrophy, are characteristic of STGD. The end-stage fundus appearance is characterized by extensive RPE and choriocapillaris atrophy, with resorbed flecks and sparse pigmentation.⁵ Peripapillary retina and RPE sparing is a diagnostic feature of STGD, even in advanced stages.⁶

Peripapillary retina sparing (absence of flecks around the optic disc) is a well-known characteristic of STGD. However, Newman et al.⁷ reported that significant defects in the peripapillary retinal nerve fiber layer (RNFL) are observed during fundus examinations of hereditary retinal dystrophy patients including STGD, which primarily affect photoreceptors and/or the RPE. Accurate detection of wedge-shaped RNFL defects on fundus examination is challenging in the presence of widespread RPE atrophy. With the clinical use of spectral-domain optical coherence tomography (SD-OCT), it is possible to evaluate the structural integrity of the RNFL, RPE, and photoreceptor layer *in vivo*. Recent studies have reported peripapillary retinal nerve fiber layer (pRNFL) loss measured by SD-OCT in hereditary retinal dystrophies, including X-linked juvenile retinoschisis, as well as autosomal recessive cone-rod dystrophy and autosomal recessive retinitis pigmentosa, both associated with ABCA4 gene mutations.⁸⁻¹⁰

The aim of this study is to evaluate pRNFL thickness in Stargardt disease using SD-OCT and to analyze its consistency with previously reported pRNFL defects in Stargardt patients.

METHODS

Between 2014 and 2022, 20 eyes from 10 patients diagnosed with STGD at our clinic, either through referral or during their initial examination, were included in this single-center, cross-sectional, case-control study along with 20 eyes from 10 age-matched healthy individuals. The study was conducted with the permission of the Ethics Committee of Health Sciences University, Dışkapı Yıldırım Beyazıt Training and Researches Hospital (Date: 22.06.2020, Decision No: 90/14). The study was performed in accordance with the tenets of the Declaration of Helsinki, and written informed consent was obtained from all participants. The stage of disease was graded according to the Fishman STGD classification.¹¹ Stage (S) 1 is characterized by macular pigmentary changes (ranging from faint/irregular pigment mottling to beaten-bronze appearance to atrophy) and irregular pigmented lesions (flecks) within one disc diameter of the fovea. These yellowish pigmented lesions can merge to form pisciform (fishtail-shaped), reticular, or branching structure. S2 is defined by yellow-white flecks that extend beyond the vascular arcades temporally and often extend nasally to the optic disc but are always confined posterior to the equator. S3 is identified by the resorption of previously observed flecks, resulting in focal atrophy of the choriocapillaris and RPE in the macula. Lastly, in S4, diffusely resorbed flecks and extensive atrophy of the choriocapillaris and RPE are observed throughout the fundus. None of the patients had evidence of acquired or hereditary systemic disease in their medical records or ophthalmological examinations. To quantify RNFL changes independent of potentially concurrent ocular diseases, patients with a history of glaucoma, increased intraocular pressure (IOP) ≥ 21 mmHg, optic neuropathy, congenital optic nerve anomalies, uveitis, any retinal diseases other than STGD, or a history of intraocular surgery (except for uncomplicated cataract extraction) were excluded from the study. Patients with a refractive error exceeding ± 5 diopters (D) sphere or ± 2 D cylinder, as well as eyes with poor OCT image quality, were also excluded.

All patients underwent a complete ocular examination, including best-corrected visual acuity (BCVA) measurement using a Snellen chart (converted to logMAR during data analysis), intraocular pressure (IOP) measurement with

Goldmann applanation tonometry, slit-lamp biomicroscopy, and dilated fundus examination using a 90 D lens. Additionally, color fundus photography, fundus autofluorescence (FAF) imaging, fundus fluorescein angiography (FFA), and macular SD-OCT (Spectralis; Heidelberg Engineering GmbH, Heidelberg, Germany) were performed.

The Spectralis SD-OCT has an axial resolution of 3.9 micrometers (μm) and scans 40,000 A-scans per second. For pRNFL measurements, an RNFL examination protocol was used for scan acquisition. The software automatically measures the RNFL by detecting Bruch's membrane opening (BMO) to determine the optic disc (OD) center and creates a calculation circle with a diameter of 3.45 mm around the OD center, following pupil dilation with 1% cycloplegia.¹² Various studies highlight the importance of fovea-disc (FoDi) alignment in pRNFL thickness measurements.¹³ Measurements based on the axis between the fovea and the center of the optic disc, as determined by the BMO, provide more accurate assessments of optic nerve head and pRNFL thickness.¹⁴ In this study, detection of the fovea using SD-OCT and performing measurements based on the anatomical axis connecting the fovea to the optic disc center were emphasized. Patients who did not meet these criteria were excluded. The RNFL thickness for each 90° quadrant (temporal, superior, nasal, and inferior) and the average thickness of all quadrants (global) were recorded in micrometers (μm) for both the case and the control groups. Then, the data were analyzed by matching individuals based on age.

The pRNFL thickness was measured at least three times in each eye on the same day and data were used only if measurements were reproducible in at least two-thirds of the acquisitions. For patients with inconsistencies in all three initial measurements, the scan was repeated three additional times, and their data were included in the study if at least two-thirds of the new measurements were consistent. Since only eyes with high-quality imaging were included in the study, there were no segmentation errors, and no manual corrections needed to be made.

Statistical Analysis

All statistical analyses were performed using SPSS software. For descriptive data analysis, the mean, standard deviation (SD), and 95% confidence interval (95%CI) were calculated. Spearman's correlation coefficient (ρ) was used to analyze the correlation between the stage of the disease and disease duration (the time from the diagnosis of STGD to the age at which the patient was included in the study).

RESULTS

A total of 20 eyes from 10 STGD patients (6 females and 4 males) with an average age of 40.9 years (range, 18–59 years) were analyzed. The control group included 20 eyes from 10 healthy individuals (6 females and 4 males), with an average age of 40.6 years (range, 19–59 years). Among these patients, the earliest age of initial diagnosis was 14 years, the latest was 47 years, and the average age of initial diagnosis was 30 years. **Table 1** presents detailed information about the patients with STGD. The IOP for all patients at the time of the study was between 12-20 mmHg (mean 16.1 mmHg). In the control group, the IOP ranged from 10 to 18 mmHg (mean 15.9 mmHg). According to the Fishman STGD classification, 10

eyes from five patients were classified as S1, eight eyes from four patients as S2, and two eyes from one patient as S3. **Figure 1** shows multimodal imaging of a Stargardt patient classified as S2. None of the patients were classified as S4 in the study. Disease stage and duration were also correlated. ($\rho=0.66$, $p=0.037$) **Figure 2** shows an example of pRNFL thickness analysis for the right eye of a STGD patient included in the study.

Table 1. Clinical data of the STGD patients in the study group

Patient no	Age (years)	Onset (years)	Gender	BCVA OD logMAR	BCVA OS logMAR	Fishman STGD classification
1	18	14	M	0,5	1	1
2	34	31	F	0,5	0,5	1
3	42	32	F	1.1	1	1
4	52	47	F	0,7	1	1
5	59	45	M	1	1	1
6	25	20	M	0,4	0,5	2
7	30	18	F	1	1	2
8	43	23	F	0,7	1,1	2
9	51	34	F	0,7	0,7	2
10	55	36	M	0,9	1	3

STGD: Stargardt disease, F/M: Female/male, BCVA: Best-corrected visual acuity, OD/OS: Right eye/left eye

The pRNFL thickness of each patient was compared to an age-matched healthy individual. Differences in pRNFL thickness for each quadrant are shown in **Figure 3**. In the temporal quadrant, 14 of 20 eyes showed thinner pRNFL (T: mean $-7.55 \mu\text{m}$, 95% CI -3 to $-12 \mu\text{m}$, 10% thinner compared to the control group), while in the nasal quadrant, pRNFL was thicker in 13 of 20 eyes (N: mean $6.85 \mu\text{m}$, 95% CI $1-13 \mu\text{m}$, 9% thicker than the control group). There were no statistically significant differences in global pRNFL thickness (G: mean $-0.75 \mu\text{m}$, 95% CI -6 to $5 \mu\text{m}$), superior quadrant thickness (S: mean $3.65 \mu\text{m}$, 95% CI -8 to $15 \mu\text{m}$) or inferior quadrant thickness (I: mean $-6 \mu\text{m}$, 95% CI -16 to $4 \mu\text{m}$) when compared with the control group.

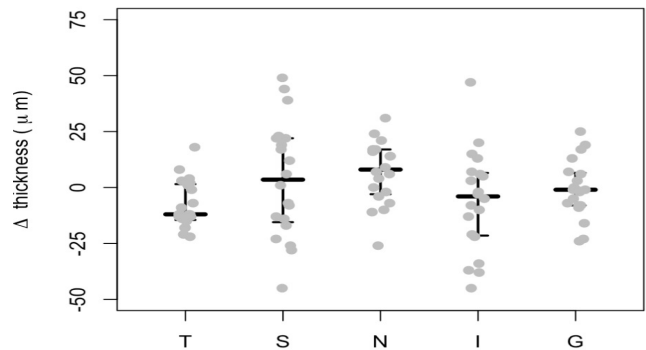


Figure 3. Differences in pRNFL thickness (Δ thickness) between Stargardt patients and the control group are shown for each quadrant (temporal, superior, nasal, and inferior) and the global (the average thickness of all quadrants). Each patient was compared with an age-matched healthy individual.

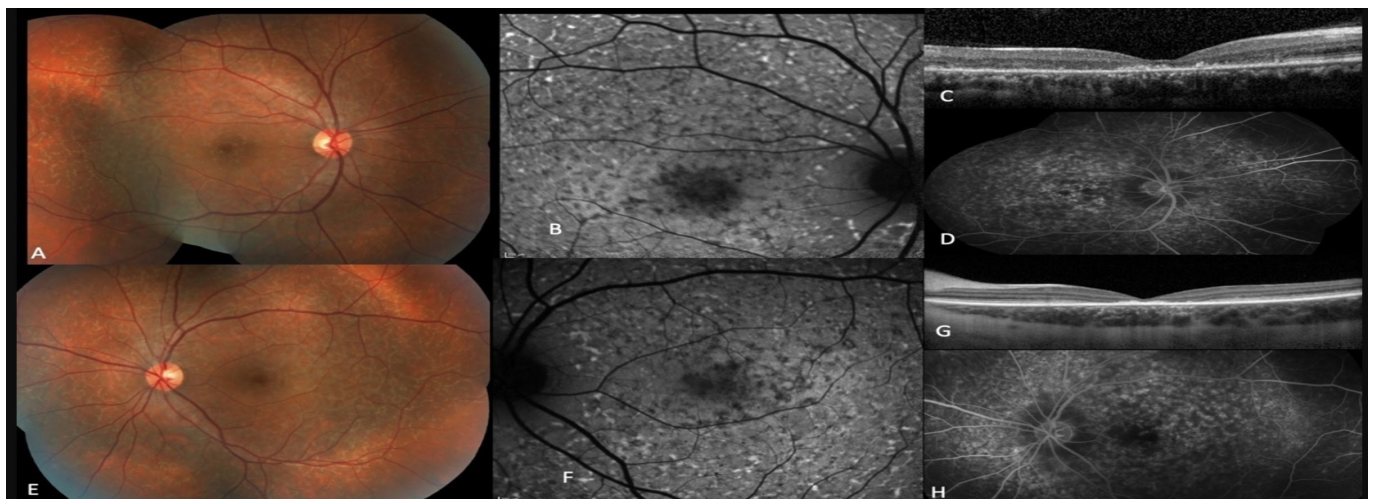


Figure 1. Multimodal imaging of a Stargardt patient classified as E2. Color fundus photographs of the right and left eyes reveal widespread yellow flecks extending beyond the vascular arcades temporally and nasally towards the optic disc, along with irregular pigment epithelial changes in the macula (A, E). In the FAF images, while the peripapillary area is spared bilaterally, flecks scattered across the posterior pole show hypoautofluorescence, whereas areas with localized RPE atrophy appear hypoautofluorescent (B, F). Horizontal line scans from SD-OCT of both eyes show lipofuscin accumulation in the RPE and disorganization in the photoreceptor layer (C, G). FFA demonstrates choroidal hypofluorescence due to lipofuscin accumulation in the RPE, along with a 'dark choroid' that allows better visualization of the retinal circulation and highlights hyperfluorescent flecks in both eyes (D, H).

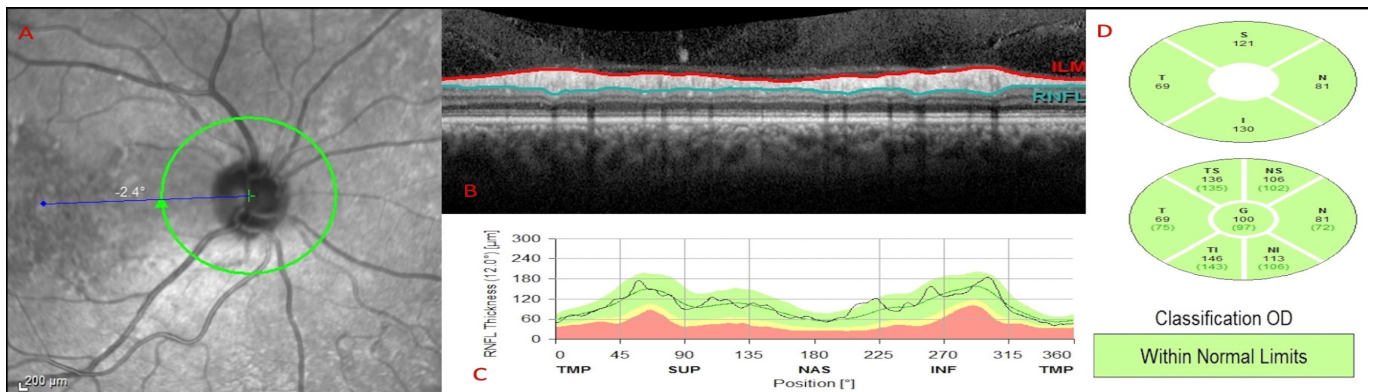


Figure 2. Measurement of pRNFL thickness using OCT in a Stargardt patient. A) Infrared fundus image showing the calculation circle with a diameter of 3.45 mm around the optic disc center (green circle) and the anatomical axis connecting the fovea to the optic disc center (blue line). The FoDi angle is observed as -2.4° . B) Circumferential OCT scan of the peripapillary retina along the calculation circle shows no segmentation errors. C) The quantification of RNFL thickness, plotted against the position along the peripapillary OCT scan (in degrees) is presented. D) The quantification of pRNFL thickness by quadrant and clock-hour sectors is shown in the pie chart with black numbers.

Table 2. Peripapillary RNFL thickness in Stargardt patients and the control group

	All Eyes n=20 (mean±SD)		Stage 1 n=10 (mean±SD)		Stage 2 n=8 (mean±SD)		Stage 3 n=2 (mean±SD)	
	Patient Group	Control Group	Patient Group	Control Group	Patient Group	Control Group	Patient Group	Control Group
Temporal, μm	67,6±9	75,2±5	64,5±9	76,7±6	67,6±7	74,5±4	83,5±5	70,5±2
Superior, μm	132,4±23	128,8±12	122,7±14	131,2±16	136,1±26	124±6	166±6	135,5±6
Nasal, μm	79,6±10	72,7±9	77,6±9	71,6±11	79,1±9	70,8±4	91,5±15	86±7
Inferior, μm	121,4±17	127,6±15	115,9±15	131,8±19	119,8±11	123,6±11	155,5±13	122±6
Global, μm	100,2±11	101±8	95,2±3	102,8±10	100,6±12	98,2±4	124±4	103±1

n: Number of eyes in the patient group, SD: Standard deviation, RNFL: Retinal nerve fiber layer

The mean pRNFL thickness of each quadrant and the global for both STGD patients at different stages and the control group, is listed in Table 2. Figure 4 illustrates the distribution of pRNFL thickness between the STGD and control groups.

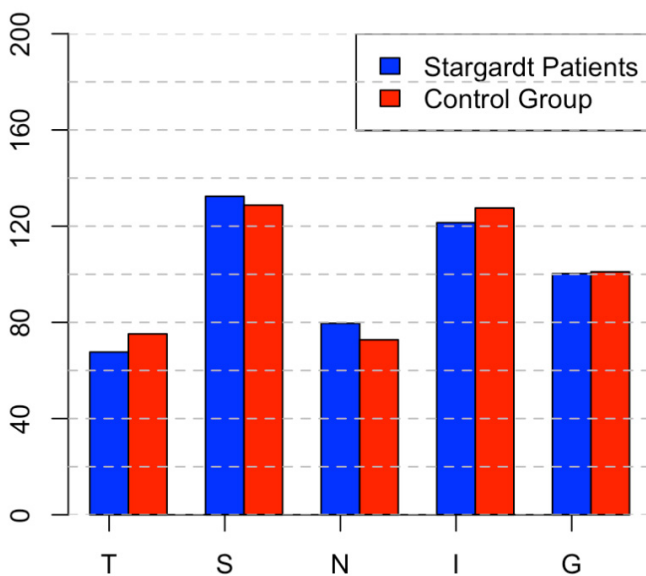


Figure 4. Distribution of pRNFL thickness (in micrometers) between Stargardt patients and the control group

DISCUSSION

Axonal loss in the peripapillary RNFL can be observed in progressive neurodegenerative optic neuropathies such as glaucoma, which is characterized by damage to retinal ganglion cells (RGCs) and their axons. It can also occur in ischemic, inflammatory, and compressive optic neuropathies.¹⁵⁻¹⁷ While pRNFL thickness analysis is important for diagnosing and monitoring the progression of these pathologies, studies have also reported that axonal damage in the RNFL can occur in macular diseases that accompany optic nerve pathologies, potentially affecting pRNFL analysis. Law et al.¹⁸ reported that advanced stages of age-related macular degeneration (AMD) are associated with thinner peripapillary RSLT, and that defects, particularly in the inferior quadrant, complicate glaucoma evaluation. In another study that included 76 eyes with dry AMD, the thickness of the macular ganglion cell-inner plexiform layer and pRNFL was thinner compared to 76 healthy eyes, with the most prominent difference observed in the temporal quadrant of the pRNFL. This preferential thinning of the papillomacular fiber bundle is explained by the fact that the axons of RGCs within the macular region are assumed to be located mainly in the temporal sectors of the optic nerve head, and the temporal pRNFL is less susceptible to glaucomatous damage than the superior and inferior quadrants. Although

the outer retinal layers are primarily affected in AMD, it has been suggested that inner retinal neurons may be affected secondarily due to photoreceptor degeneration.¹⁹ Additionally, in rat models of retinal degeneration, histochemical changes in both the inner plexiform layer and the RGC layer have been attributed to photoreceptor cell damage.²⁰ To quantify pRNFL changes resulting from macular diseases independently of potentially coexisting optic nerve pathologies, it is reasonable to focus on hereditary macular dystrophies, which are typically seen in younger individuals. Pasadhika et al.⁹ reported that in a study of 11 patients with cone-rod dystrophy, thinning of the pRNFL was observed in 8 patients, most prominently in the temporal quadrant. They suggested that, the inner retinal layers can also be affected in degenerative retinal diseases that primarily affect the outer retinal layers. Their study proposed that this might result from either transsynaptic degeneration or, as yet unidentified mechanisms by which photoreceptor cell degeneration directly affects the inner retinal layers.⁹ In retinitis pigmentosa (RP), characterized by progressive degeneration of photoreceptor cells and the RPE, it has been proposed that damage to the outer retinal layers leads to transneuronal changes resulting in RGC loss.⁷ Stone et al.²¹ have shown a relationship between the loss of photoreceptor cells and transneuronal ganglion cell death. Another study performed on the retinas of human retinitis pigmentosa donors with intermediate and advanced stages of RP showed a loss of the inner nuclear layer and retinal ganglion cell layer, as well as a reduction in the number of RGCs.²² Reports in the literature indicate that hereditary retinal dystrophies, including Stargardt disease, are primarily characterized by photoreceptor and/or RPE dysfunction, thinning of the inner retinal layers, and defects in the pRNFL.^{7,23} However, pRNFL thickness analysis specifically in STGD has been reported in only two studies to date. Genead et al.²⁴ reported that, among 27 patients with STGD, thinning of the pRNFL was observed in one or more quadrants in 24 eyes (46.2%) from 14 patients (51.9%). The distribution of abnormal thinning was noted as follows: 33.3% in the superior quadrant, 33.3% in the inferior quadrant, 16.7% in the nasal quadrant, and 16.7% in the temporal quadrant.²⁴ This distribution is noteworthy considering that STGD primarily affects the macula with the papillomacular bundle corresponding to the temporal quadrant, especially when compared to studies related to hereditary retinal dystrophies mentioned above. Reich et al.²⁵ reported that in their study of 20 Stargardt patients (39 eyes), thinning of the pRNFL in the temporal quadrant was detected in 36 of 39 eyes, with the mean pRNFL thickness in the temporal quadrant being 16% thinner than the control group. This study highlighted the importance of manually correcting the fovea-optic disc (FoDi) angle when evaluating pRNFL thickness using OCT. In cases where automatic software detection of the fovea failed due to macular

atrophy, Reich et al.²⁵ manually corrected the fovea-optic disc (FoDi) axis in 11 patients (15 eyes) and presented the results before correction. Before correcting the FoDi axis, thinning of the pRNFL was detected in one or more quadrants in 17 eyes (43.6%) of 11 patients (55%), with thinning observed in 54% of the inferior quadrant, 33.5% of the temporal quadrant, and 12.5% of the superior quadrant. This distribution was consistent with the findings reported by Genead et al.²⁴ Since Genead et al. did not describe corrections for misalignments in RNFL measurements relative to the fovea, Reich et al. suggested that the observed thinning in the inferior quadrant might be due to errors in fovea detection, emphasizing the importance of the FoDi angle in improving the reliability of pRNFL thickness analysis. In previous studies, mean FoDi angle values range between -5.6° and -7.7° and the FoDi distribution is between -17° (the fovea is 17° below the disc) and $+7^\circ$ (the fovea is 7° above the disc).¹⁵ To remain consistent with the literature, our study ensured that measurements adhered to these FoDi angle values. Patients in whom the fovea was not correctly detected or whose measurements were not aligned with the anatomical axis connecting the fovea and the optic disc center were excluded from the analysis. In 70% of the eyes, thinning of the pRNFL was observed in the temporal quadrant, which was 10% thinner than that in the control group, supporting the findings of Reich et al. Since the correct alignment of the FoDi axis has no influence on the global RNFL, no significant differences were observed in our study, similar to the results reported in Reich et al.²⁵ and Genead et al.²⁴

Primary neuronal injury affects distal neurons, a process known as transsynaptic or transneuronal degeneration, which can be divided into anterograde and retrograde based on the site of origin and direction of spread.²⁶ Reich et al.²⁵ proposed that RGC loss resulting from photoreceptor cell damage may be due to anterograde transsynaptic axonal degeneration. This degeneration is described as 'dying-forward,' where the postsynaptic neuron is affected by damage to the presynaptic neuron. This process is believed to be caused by defective afferent innervation, reduced transmission of growth and survival factors from the supplying cell.^{25,27} Furthermore, it has been reported that in glaucoma, damage starting in the RGCs initiates a transneuronal degeneration chain, which affects both the outer retinal layers and the visual cortex.^{26,28} Although the confidence interval is wider compared to the results of Reich et al.²⁵ we also detected increased RNFL thickness in the nasal quadrant, where the photoreceptor cells are still functional. Given that STGD primarily affects the macula, but in advanced stages, RPE and photoreceptor loss extend beyond the macula toward the nasal side of the optic disc, thinning of the pRNFL in the temporal quadrant is expected, whereas the nasal quadrant might not show RSLT loss. RPE plays a key role in RGC neurogenesis through the Wnt and Numb/Notch signaling pathways. Therefore, it is possible that impaired signaling early in development due to dysfunctional RPE may lead to a prolonged period of ganglion cell neurogenesis, potentially resulting in increased RNFL thickness.²⁹ In Stargardt disease, where sparing of the peripapillary retina and RPE is considered pathognomonic, recent studies have shown that flecks and RPE atrophy can also be observed in the peripapillary retina.^{30,31} These findings were not detected in the imaging of our patient group. Although our study included a sex- and age-matched control group, one of its limitations is the relatively small number of patients. In advanced stages

of STGD, further RNFL loss is expected as atrophy extends beyond the macula.

Limitations

Among the patients, only one was classified as S3 according to the Fishman classification, and no patient was classified as S4. As a result, the extent of pRNFL loss in advanced stages and the correlation between the stage and the extent of pRNFL loss could not be investigated. In addition, our study lacked longitudinal follow-up data. Given these limitations, further multicenter studies with larger patient cohorts, including those in advanced stages and with long-term follow-up are needed for comprehensive analysis of pRNFL in STGD.

CONCLUSION

STGD, characterized by RPE atrophy and photoreceptor cell loss in the macula, shows thinning in the temporal quadrant of the pRNFL, corresponding to the papillomacular nerve fiber bundle, which consists of axons of the RGCs from the fovea and nasal macula. It is not yet clear whether the loss of RNFL is due to transneuronal degeneration or an as-yet-undefined mechanism where the degeneration of outer retinal layers directly affects the inner retinal layers, potentially involving retinal remodeling.

ETHICAL DECLARATIONS

Ethics Committee Approval

The study was conducted with the permission of the Ethics Committee of Health Sciences University, Dışkapı Yıldırım Beyazıt Training and Research Hospital (Date: 22.06.2020, Decision No: 90/14).

Informed Consent

All patients signed and free and informed consent form.

Referee Evaluation Process

Externally peer-reviewed.

Conflict of Interest Statement

The authors have no conflicts of interest to declare.

Financial Disclosure

The authors declared that this study has received no financial support.

Author Contributions

All of the authors declare that they have all participated in the design, execution, and analysis of the paper, and that they have approved the final version.

REFERENCES

- Garces F, Jiang K, Molday LL, et al. Correlating the expression and functional activity of ABCA4 disease variants with the phenotype of patients with Stargardt disease. *Invest Ophthalmol Vis Sci.* 2018;59(6):2305-2315.
- Raj RK, Dhoble P, Anjanamurthy R, et al. Genetic characterization of Stargardt clinical phenotype in South Indian patients using Sanger and targeted sequencing. *Eye Vis (Lond).* 2020;7(1):1-10.
- Sparrow JR, Fishkin N, Zhou J, et al. A2E, a byproduct of the visual cycle. *Vision Res.* 2003;43(28):2983-2990.
- Lugo-Merly A, Thurin LJM, Izquierdo-Encarnacion NJ, Casillas-Murphy SM, Oliver-Cruz A. Stargardt disease due to an intronic mutation in the ABCA4: a case report. *Int Med Case Rep J.* 2022;15:693-698.

5. Battaglia Parodi M, Cicinelli MV, Rabiolo A, Pierro L, Bolognesi G, Bandello F. Vascular abnormalities in patients with Stargardt disease assessed with optical coherence tomography angiography. *Br J Ophthalmol*. 2017;101(6):780-785.
6. Nassisi M, Mohand-Said S, Andrieu C, et al. Peripapillary sparing with near infrared autofluorescence correlates with electroretinographic findings in patients with Stargardt disease. *Invest Ophthalmol Vis Sci*. 2019; 60(15):4951-4957.
7. Newman NM, Stevens RA, Heckenlively JR, Francisco S. Nerve fibre layer loss in diseases of the outer retinal layer from the departments of ophthalmology of the Pacific Presbyterian Medical Center. *Invest Ophthalmol Vis Sci*. 1987;71(1):21-26.
8. Walia S, Fishman GA. Retinal nerve fiber layer analysis in RP patients using Fourier-domain OCT. *Invest Ophthalmol Vis Sci*. 2008;49(8):3525-3528.
9. Pasadhika S, Fishman GA, Allikmets R, Stone EM. Peripapillary retinal nerve fiber layer thinning in patients with autosomal recessive cone-rod dystrophy. *Am J Ophthalmol*. 2009;148(2):260-265.e1.
10. Genead MA, Pasadhika S, Fishman GA. Retinal nerve fibre layer thickness analysis in X-linked retinoschisis using Fourier-domain OCT. *Eye*. 2009; 23(5):1020-1027.
11. Fishman GA. Fundus flavimaculatus: a clinical classification. *Arch Ophthalmol*. 1976;94(12):2061-2067.
12. Abe RY, Medeiros FA. The use of spectral-domain optical coherence tomography to detect glaucoma progression. *Open Ophthalmol J*. 2015;9: 78-88.
13. Tuncer Z, Erdurman C. Does foveal position relative to the optic disc affect optical coherence tomography measurements in glaucoma? *Turk J Ophthalmol*. 2018;48(4):178-184.
14. Chauhan BC, Burgoyne CF. From clinical examination of the optic disc to clinical assessment of the optic nerve head: a paradigm change. *Am J Ophthalmol*. 2013;156(2):218-227.e2.
15. Weinreb RN, Aung T, Medeiros FA. The pathophysiology and treatment of glaucoma: a review. *JAMA*. 2014;311(18):1901-1911.
16. Fisher JB, Jacobs DA, Markowitz CE, et al. Relation of visual function to retinal nerve fiber layer thickness in multiple sclerosis. *Ophthalmology*. 2006;113(2):324-332.
17. Dotan G, Goldstein M, Kesler A, Skarf B. Long-term retinal nerve fiber layer changes following nonarteritic anterior ischemic optic neuropathy. *Clin Ophthalmol*. 2013;7:735-740.
18. Law SK, Small KW, Caprioli J. Peripapillary retinal nerve fiber measurement with spectral-domain optical coherence tomography in age-related macular degeneration. *Vision (Basel)*. 2017;1(4):26.
19. Lee EK, Yu HG. Ganglion cell-inner plexiform layer and peripapillary retinal nerve fiber layer thicknesses in age-related macular degeneration. *Invest Ophthalmol Vis Sci*. 2015;56(6):3976-3983.
20. Lund RD, Coffey PJ, Sauve Y, Lawrence JM. Intraretinal transplantation to prevent photoreceptor degeneration. *Ophthalmic Res*. 1997;29(5):305-319.
21. Stone JL, Barlow WE, Humayun MS, De Juan E, Milam AH. Morphometric analysis of macular photoreceptors and ganglion cells in retinas with retinitis pigmentosa. *Arch Ophthalmol*. 1992;110(11):1634-1639.
22. Santos A, Humayun MS, De Juan E, et al. Preservation of the inner retina in retinitis pigmentosa: a morphometric analysis. *Arch Ophthalmol*. 1997;115(4):511-515.
23. Lim JJ, Tan O, Fawzi AA, Hopkins JJ, Gil-Flamer JH, Huang D. A pilot study of Fourier-domain optical coherence tomography of retinal dystrophy patients. *Am J Ophthalmol*. 2008;146(3):417-426.
24. Genead MA, Fishman GA, Anastakis A. Spectral-domain OCT peripapillary retinal nerve fiber layer thickness measurements in patients with Stargardt disease. *Br J Ophthalmol*. 2011;95(5):689-693.
25. Reich M, Lübke J, Joachimsen L, et al. Thinner temporal peripapillary retinal nerve fibre layer in Stargardt disease detected by optical coherence tomography. *Invest Ophthalmol Vis Sci*. 2021;259(6):1521-1528.
26. You M, Rong R, Zeng Z, Xia X, Ji D. Transneuronal degeneration in the brain during glaucoma. *Front Aging Neurosci*. 2021;13:643685.
27. Herro AM, Lam BL. Retrograde degeneration of retinal ganglion cells in homonymous hemianopsia. *Clin Ophthalmol*. 2015;9:1057-1064.
28. Lei Y, Garrahan N, Hermann B, et al. Quantification of retinal transneuronal degeneration in human glaucoma: a novel multiphoton-DAPI approach. *Invest Ophthalmol Vis Sci*. 2008;49(5):1940-1945.
29. Fu DJ, Xue K, Jolly JK, MacLaren RE. A detailed in vivo analysis of the retinal nerve fibre layer in choroideremia. *Acta Ophthalmol*. 2019;97(4):e589-e600.
30. Jayasundera T, Rhoades W, Branham K, Niziol LM, Musch DC, Heckenlively JR. Peripapillary dark choroid ring as a helpful diagnostic sign in advanced Stargardt disease. *Am J Ophthalmol*. 2010;149(4):656-660.e2.
31. Burke TR, Allikmets R, Smith RT, Gouras P, Tsang SH. Loss of peripapillary sparing in non-group I Stargardt disease. *Exp Eye Res*. 2010;91(5):592-600.